



The Flow Behavior of Molten Steel in an RH Degasser Under Different Ladle Bottom Stirring Processes

RUDONG WANG, YU JIN, and HENG CUI

The effects of the ladle bottom stirring flow rate and the number of argon plugs on the circulation flow rate and mixing time in an RH degasser were studied using a physical simulation method. The flow field in the RH ladle was studied using particle image velocimetry (PIV). The results show that applying the ladle bottom stirring process has a great influence on the flow field in the RH ladle. When only stirring under the upleg, the circulation of the RH ladle was enhanced. The velocity of molten steel circulation was accelerated, the RH circulation flow rate was increased, and the mixing time was decreased. When the lifting gas flow rate is $133.3 \text{ m}^3 \text{ h}^{-1}$ and the ladle bottom stirring rate is 166.7 L min^{-1} , the circulation flow rate increases by approximately 25 pct, and the mixing time decreases between 36 and 40 pct compared with that without ladle bottom stirring. Stirring in the argon plug below the downleg is not conducive to improving the circulation flow rate but is beneficial to reducing the molten steel mixing time. Double-ladle argon plug stirring can improve molten steel activity on both sides of the snorkel at the upper part of the RH ladle, but this can negatively affect the original vessel circulation. To ensure that the circulation flow is not reduced during double-ladle bottom argon plug stirring, the snorkel upleg lifting gas flow rate must be greater than $133.3 \text{ m}^3 \text{ h}^{-1}$ for the system studied in this work.

<https://doi.org/10.1007/s11663-021-02371-8>

© The Minerals, Metals & Materials Society and ASM International 2021

I. INTRODUCTION

THE Ruhrstah–Heraeus (RH) refining unit has been widely used in the secondary refining process of steel production. The RH refining unit provides functionality for decarburization, degassing, uniformity composition and temperature, and the promotion of inclusion floating. The flow in the RH refining unit occurs under vacuum conditions. The molten steel flows upward under the action of bubble buoyancy, and the molten steel circulates between the vacuum chamber and the ladle through two snorkels. The circulation flow of molten steel in the RH refining process is also the basis and core of various physical and chemical reactions. The flow of molten steel in the RH refining unit significantly affects the RH refining efficiency. Therefore, the study of the RH internal flow field is of great significance.

There are many ways to improve the circulation flow rate, but there are limits. In a study by Mukherjee *et al.*,^[1] it was found that increasing the lifting gas flow rate generally increases the circulation flow rate. There is an optimal value beyond which the circulation flow rate decreases. The increase in snorkel immersion depth can improve the circulation flow rate. However, in actual production, if the immersion depth is too deep, the molten steel will overheat the bottom of the vacuum chamber and reduce the service life of the vacuum chamber. Reducing the pressure of the vacuum chamber can also increase the circulation flow. Zhu *et al.*^[2] used a numerical simulation method to find that the circulation flow rate increases with the increase in lifting gas flow rate in the upleg, but when the lifting gas flow rate reaches a certain value, the circulation flow rate of liquid steel slows down. In the research of Kishan *et al.*^[3] and Li *et al.*,^[4] the circulation flow rate could be increased to a limited extent using a multisnorkel system (single upleg and double downleg). Using a numerical simulation and physical simulation, Luo *et al.*^[5] found that compared with a traditional structure, an elliptical downleg could increase the circulation flow rate and reduce the scouring of molten steel on the ladle lining. In recent years, more comprehensive studies have been conducted on the RH process. Nevertheless, due to the limitations of the production equipment conditions

RUDONG WANG and HENG CUI are with the Collaborative Innovation Center of Steel Technology, University of Science and Technology Beijing, Beijing, 100083, P.R. China. Contact e-mail: cuiheng@ustb.edu.cn YU JIN is with the China National Institute of Standardization, Beijing, 100191, P.R. China.

Manuscript submitted April 20, 2021; accepted October 29, 2021.

Article published online November 15, 2021.

(such as the vacuum chamber diameter and the ladle size), the increase in the circulation flow rate is limited. Therefore, it is necessary to investigate other measures to improve the circulation flow rate.

Da Silva *et al.*^[6] used a physical simulation method to study the effect of ladle bottom stirring under an upleg on the RH mixing time and confirmed the effectiveness of gas injection at the bottom of the ladle. Chen *et al.*^[7] used a numerical simulation method to study the RH mixing behavior in single argon plug stirring and triple-ladle argon plug stirring processes. Argon stirring below the upleg can improve the circulation flow rate, and adding another two bottom stirrers at appropriate positions can further shorten the mixing time. Geng *et al.*^[8] used a numerical method to investigate the flow field and the mixing characteristics in an RH degasser with ladle bottom stirring to find the optimal bottom stirring location to achieve a large circulation flow rate and small mixing time. He *et al.*^[9] used a coupled volume of fluid method—discrete phase model of numerical simulation to study the effect of ladle bottom gas injection on the mixing characteristic and slag layer behaviors in an RH unit. Their results showed that the optimal injection location to obtain the shortest mixing time and avoid the formation of slag eyes is under the upleg. Zhang *et al.*,^[10] Zhang *et al.*^[11] and Ling *et al.*^[12] used particle imaging velocimetry (PIV) to measure the flow field of an RH degasser using a water model. All the above research provides new ideas and methods for the research of RH degassers. Nevertheless, there is a lack of systematic research on the flow behavior of liquid steel in RH degasser bottom stirring using a physical simulation method.

In this paper, a water model is established based on the similarity principle. A physical simulation method and PIV technology are used to study the influence of process parameters such as the number of bottom argon plug stirring locations, the bottom stirring flow rate, the lifting gas flow rate, the snorkel immersion depth, and the vacuum chamber pressure on the flow behavior in an RH degasser and ladle. The goal of this work is to provide a theoretical basis for determining the appropriate process and operational parameters.

II. EXPERIMENTAL PROCEDURE

A. Physical Modeling

A water model was designed based on an industrial 150-ton RH degasser with a similarity ratio of 1:4. The size parameters of the prototype and the model are shown in Table 1. A schematic diagram of the RH degasser model is shown in Figure 1. The top view of the industrial RH ladle bottom is shown in Figure 2. The bottom ladle gas injection plug 1 (location 1) is located under the upleg, and the bottom ladle gas injection plug 2 (location 2) is located below the downleg side. The pressure in the vacuum chamber in the model was measured with a U-type pressure gauge.

The liquid steel flow in the RH degasser is mainly affected by viscous force, gravity, and inertia force. To ensure the accuracy of the physical model simulation, in addition to ensuring the model's geometric similarity, it is also necessary to ensure that the Reynolds number (Re) and modified Freud number (Fr) satisfy similarity requirements. In the RH degasser system, the Reynolds number of the model and the prototype are in the second modeling zone (turbulent regime).^[13] The turbulent Reynolds number similarity criterion is naturally satisfied if one operates in the turbulent regime.^[14] Therefore, the dynamic similarity between the water model and the industrial prototype can be ensured by equal Fr of the two systems,^[1,6,13,15] as shown by Eq. [1]:

$$Fr = \frac{\rho_g u^2}{gD(\rho_l - \rho_g)} = \text{const} \quad [1]$$

According to Eq. [1], the equality of the Freud number between the prototype and water model is expressed in Eq. [3]. By replacing the velocity u using the right-hand side of Eq. [2] and further considering that the density of gas is much lower than that of liquid, Eq. [5] can be simplified to Eq. [4].

$$u = \frac{4Q}{\pi d^2} \quad [2]$$

$$\frac{\rho_{g,p} u_p^2}{gD_p(\rho_{l,p} - \rho_{g,p})} = \frac{\rho_{g,m} u_m^2}{gD_m(\rho_{l,m} - \rho_{g,m})} \quad [3]$$

$$\left(\frac{Q_m}{Q_p}\right)^2 = \left(\frac{1}{\lambda}\right)^5 \left(\frac{\rho_{g,p}}{\rho_{g,m}}\right) \left(\frac{\rho_{l,m}}{\rho_{l,p}}\right) \quad [4]$$

Since the gas pressure and flow rate are measured under the standard state, the gas flow rate and density are modified using the gas equation of state Eqs. [5] and [6], and the flow rate relationship between the model and the prototype under the standard state is Eq. [7].

$$Q = Q^0 \frac{P^0}{P} \frac{T}{T^0} \quad [5]$$

$$\rho = \rho^0 \frac{P}{P^0} \frac{T^0}{T} \quad [6]$$

$$\frac{Q_m^0}{Q_p^0} = \sqrt{\left(\frac{1}{\lambda}\right)^5 \left(\frac{\rho_{g,p}^0}{\rho_{g,m}^0}\right) \left(\frac{\rho_{l,m}}{\rho_{l,p}}\right) \left(\frac{T_{l,p} P_{g,m}}{T_{l,m} P_{g,p}}\right)} \quad [7]$$

According to the pressure formula Eqs. [8] and [9], the similarity of vacuum degree in the RH vacuum chamber is shown in Eq. [10].

Table I. Dimensional Parameters of the Industrial Unit and the Water Model

| Parameters | Industrial Unit | Water Model |
|---------------------------------------|-----------------|-------------|
| Inner Diameter of Ladle Top (mm) | 3160 | 790 |
| Inner Diameter of Ladle Bottom (mm) | 2862 | 715.5 |
| Ladle Height (mm) | 3850 | 962.5 |
| Inner Diameter of Vacuum Chamber (mm) | 1800 | 450 |
| Outer Diameter of Snorkel (mm) | 1200 | 300 |
| Inner Diameter of Snorkel (mm) | 550 | 137.5 |
| Length of Snorkel (mm) | 1500 | 375 |

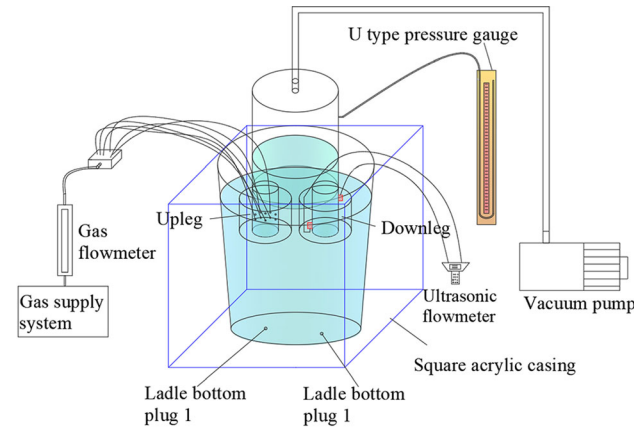


Fig. 1—Schematic of RH degasser ladle water model.

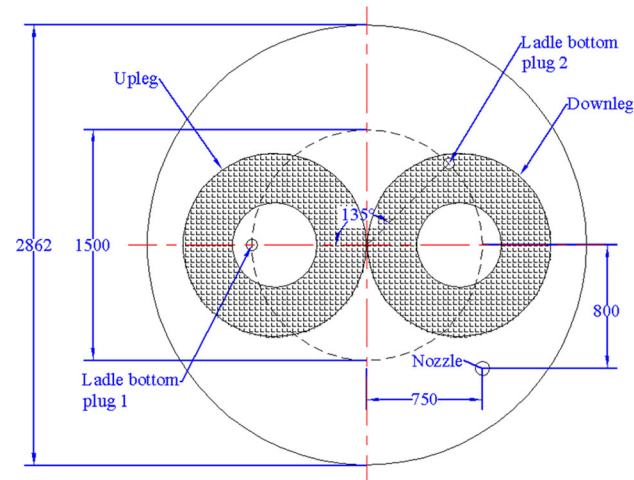


Fig. 2—Top view of the bottom of RH ladle (industrial unit). Dimensions in mm.

$$P_0 = P_{vac} + \rho_l g h_0 \quad [8]$$

$$\Delta P = P_0 - P = \rho g h_0 \quad [9]$$

$$\frac{\Delta P_m}{\Delta P_p} = \frac{\rho_{l,m} g h_{0,m}}{\rho_{l,p} g h_{0,p}} = \frac{1000}{7000} \times \frac{1}{4} = \frac{1}{28} \quad [10]$$

The operational parameters obtained from Eqs. [1] through [10] are shown in Table II.

B. Circulation Flow Rate Measurement

An ultrasonic flowmeter measured the downleg flow to characterize the RH circulation flow rate. The arrangement is shown in Figure 1, and the sensor was installed outside the downleg. According to the downleg material and size, the distance (100 mm) between the two ultrasonic flowmeter sensors was determined. For each work condition, the measurement was repeated three times, and the average was taken as the operating condition's circulation flow rate.

C. Mixing Time Measurement

The mixing time was measured by the conductivity method. A saturated KCl solution (200 ml) was added to the RH vacuum chamber as a tracer, and the water conductivity was measured. When the conductivity maintained a stable value ± 5 pct within a 15 seconds window, the RH–Vessel–Ladle system was considered to be completely mixed, and this moment was the mixing time. The acquisition time of the conductivity meter was 120 seconds, and the acquisition interval was 0.04 seconds. To reduce test errors, the measurement was repeated three times for each working condition, and an average was taken.

D. Particle Image Velocimetry (PIV)

PIV is a transient, multipoint, noncontact hydrodynamic velocity measurement method that can record the flow field information entirely at a particular time to obtain the spatial structure and flow characteristics of the ladle flow field. This experiment used LaVision® PIV equipment, which has a double 400 MJ pulse energy Nd:YAG laser, and the laser irradiates the cross-section shown in Figure 3. Hollow glass balls with a diameter of 50 μm were added to the RH water model as the tracer

particles, and two CCD cameras with a maximum resolution of 4008×2672 pixels were used to record synchronously with the laser to capture the movement of the particles in the laser film; 100 frames of photos were taken in 10.2 seconds of the RH–Degasser–Ladle system. The velocity distribution of the flow field of the ladle was obtained through calculation and analysis with Davis[®] software. The PIV system is shown in Figure 3.

Because the ladle is in the shape of a rounded truncated cone, the PIV results are distorted due to refraction. Matching index of refraction (MIR) technology can reduce the refraction of light through complex geometry by matching the refractive index of transparent materials and flowing media.^[16] As shown in Figure 3, using a square acrylic casing on the outside of the ladle can ensure that the refractive indices of the inside and outside of the ladle model are relatively close, thereby reducing the influence of light refraction on the PIV results.^[17]

III. RESULTS AND DISCUSSION

The effects of the ladle bottom stirring flow rate, lifting gas flow rate, immersion depth, and vacuum chamber pressure on the circulation flow rate, mixing time, and flow field are discussed in the following.

A. Effect of Different Ladle Bottom Stirring Parameters on the Circulation Flow Rate

The prototype parameters were as follows: the snorkel immersion depth was 500 mm, the vacuum chamber pressure was 133 Pa, and the other parameters are shown in Table II. The circulation flow rates of double-ladle argon plug stirring, single-ladle argon plug stirring location 1, and single-ladle argon plug stirring location 2 under different lifting gas flow rates and ladle bottom stirring flow rates are shown in Figure 4. The values in the figure are the converted industrial prototype parameter values, and the ladle bottom stirring flow rate of zero represents the case in which there is no bottom stirring.

In Figure 4, the circulation flow rate in RH ladle varies significantly under different bottom stirring conditions, and under the same bottom stirring condition, the RH circulation flow rate increases with an increasing lifting gas flow rate.

Under the double-ladle argon plug stirring condition, when the lifting gas flow rate is $33.3 \text{ m}^3 \text{ h}^{-1}$, the circulation flow rate decreases as the ladle bottom stirring flow rate increases. With the increase in the flow rate of the lifting gas, the circulation flow rate first increases and then decreases, and the inflection point moves to the right as the lifting gas flow increases. When the flow rate of the lifting gas increases to $100 \text{ m}^3 \text{ h}^{-1}$, with the increase in the ladle bottom stirring flow rate, the circulation flow rate first increases and then basically remains unchanged. The reason is that the driving force of RH circulation is small when the lifting gas flow is

small, and the damage of liquid steel circulation in the ladle increases with the increase in double-ladle argon plug stirring, so the circulation flow is gradually reduced. With the increase in the lifting gas flow rate, the driving force of the RH cycle increases, and the damage of ladle bottom stirring to liquid steel circulation is alleviated. With the increase in the ladle bottom stirring flow rate, the RH cycle flow rate first increases and then decreases.

Under the condition of single-ladle argon plug stirring at location 1, the circulation flow of the RH ladle increases with increasing ladle bottom stirring flow under each lifting gas flow rate. When the lifting gas flow is $33.3 \text{ m}^3 \text{ h}^{-1}$, the ladle bottom stirring flow increases to 166.7 L min^{-1} , which is approximately 37 pct higher than that without ladle bottom stirring; when the lifting gas flow is $100 \text{ m}^3 \text{ h}^{-1}$, the ladle bottom stirring flow increases to 166.7 L min^{-1} . Compared with no ladle bottom stirring, the circulation flow rate increases by approximately 25 pct. The reason is that the ladle bottom stirring under the RH upleg accelerates the circulation of liquid steel without changing the original circulation pattern of liquid steel in the ladle, and the promotion effect is more evident when the lifting gas flow is low.

The effects of single-ladle argon plug stirring at location 1 and double-ladle argon plug stirring were compared. Only when the lifting gas flow is $100 \text{ m}^3 \text{ h}^{-1}$ and each ladle bottom argon plug stirring flow is 33.3 and 66.7 L min^{-1} , the RH circulation flow of double-ladle plug stirring is greater than that of single-ladle argon plug stirring 1, and it is less than that of single-ladle argon plug stirring under other conditions. However, under these two conditions, the amount of gas injected into liquid steel by double-ladle argon plug stirring is twice that injected by single-ladle argon plug stirring 1. As shown in Figure 4, when the same amount of gas is injected, the single-ladle argon plug stirring 1 air volume is 66.7 L min^{-1} , the circulation flow rate is $135.60 \text{ t min}^{-1}$, which is slightly higher than the double-ladle argon plug stirring, the circulation is 33.3 L min^{-1} , and the circulation flow rate is $134.56 \text{ t min}^{-1}$. Therefore, from the point of view of liquid steel temperature reduction and gas consumption, single-ladle argon plug stirring 1 is better than double-ladle argon plug stirring at improving the RH circulation flow.

Under the condition of single-ladle argon plug stirring at location 2, the circulation flow decreases with increasing bottom stirring flow rate. Under all experimental conditions, the circulation flow of single-ladle argon plug stirring 2 is less than that of no bottom stirring, single-ladle argon plug stirring 1, and double-ladle argon plug stirring. Introducing single-ladle argon plug stirring 2 is not conducive to improving the circulation flow of the RH degasser. The reason is that the circulation flow in the ladle is destroyed under this condition. With the increase in the ladle bottom stirring flow rate, the destruction trend is intensified, so the circulation flow rate decreases gradually with the increase in the ladle bottom stirring flow rate.

Table II. Operational Parameters of the Industrial Unit and the Water Model

| Parameters | Industrial Unit | Water Model |
|--|-----------------|------------------------|
| Lifting Gas Flow Rate ($\text{m}^3 \text{h}^{-1}$) | 33.3 to 133.3 | 1 to 4 |
| Pressure of Vacuum Chamber (Pa) | 133/3325/6685 | 97711/97825/97945 |
| Density of the Gas (kg m^{-3}) | 1.782 (argon) | 1.292 (compressed air) |
| Density of the Liquid (kg m^{-3}) | 7000 (steel) | 1000 (water) |
| Temperature (K) | 1873 | 293 |
| Pressure in Surroundings (Pa) | 101, 325 | 101, 325 |
| Immersion Depth of the Snorkels (mm) | 400/500/600 | 100/125/150 |
| Bottom Gas Flow Rate (L min^{-1}) | 0 to 166.7 | 0 to 5 |

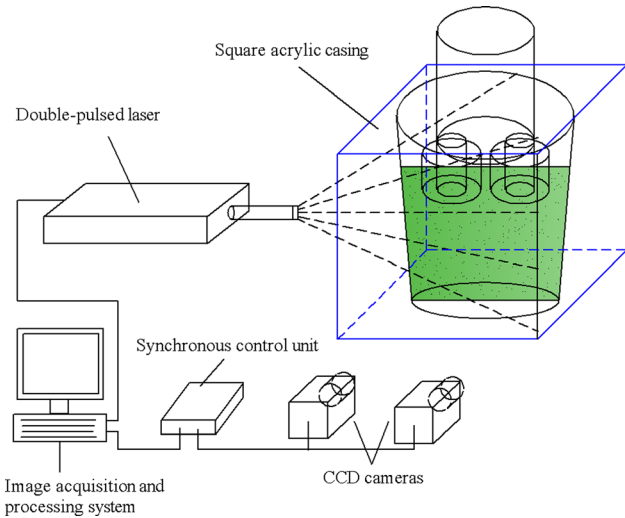


Fig. 3—Schematic of the PIV system.

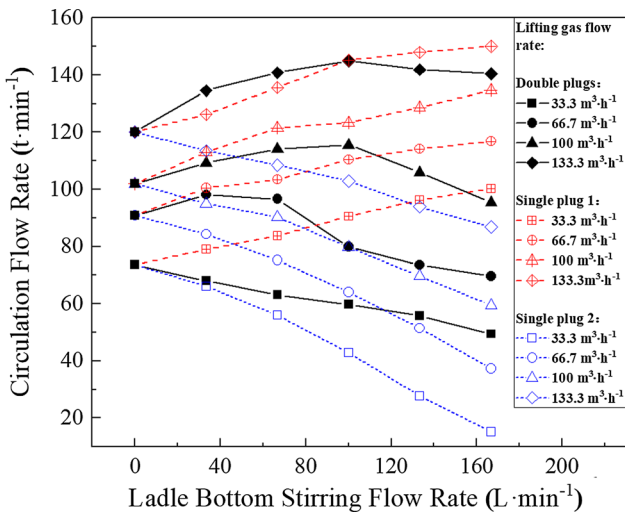


Fig. 4—Variation in circulation flow with ladle bottom stirring flow under different ladle bottom stirring conditions and lifting gas flow rates.

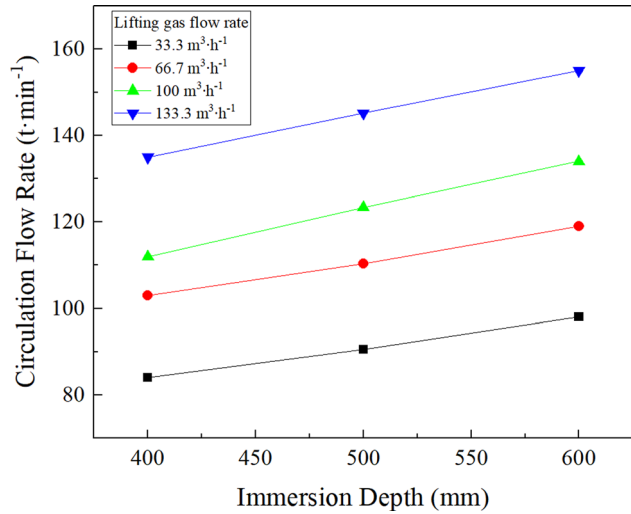


Fig. 5—Relationship between the circulation flow rate and the immersion depth of the snorkel under single-ladle argon plug stirring 1.

Compared with the case without ladle bottom stirring, the circulation flow rate increases when stirring in the ladle bottom argon plug below the upleg and decreases when stirring in the ladle bottom argon plug below the downleg. The changing trend of circulating flow rate under single plug ladle bottom stirring obtained by physical simulation is similar to the numerical simulation result of References 8 and 9. In this study, the double plug ladle bottom stirring experiment was supplemented, and the effect of double plug ladle bottom stirring on circulation flow was between that of two single plug ladle bottom stirring cases. Therefore, under several ladle bottom stirring conditions, single-ladle argon plug stirring 1 has the best effect on improving the circulation flow. Figure 5 shows the influence of immersion depth (vacuum chamber pressure is 133 Pa, ladle bottom stirring flow rate is 100 L min^{-1}) on circulation flow rate under the condition of single-ladle argon plug stirring 1. Figure 5 shows that under the condition of single-ladle argon plug stirring of 1, the circulation flow rate under different lifting gas flow rates increases with increasing immersion depth.

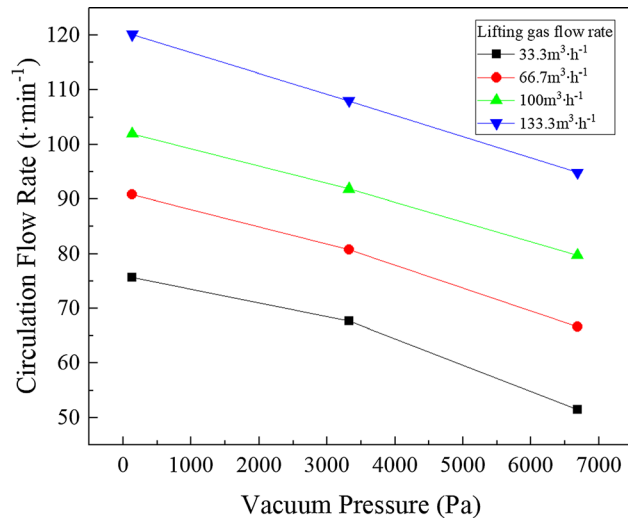


Fig. 6—Relationship between the circulation flow rate and the pressure of the vacuum chamber.

To fit the circulation flow rate formula, the relationship between the circulation flow rate and the immersion depth of the snorkel was studied. Figure 6 shows the influence of vacuum chamber pressure (immersion depth is 500 mm) on circulation flow rate under no ladle bottom stirring. The circulation flow rate under different lifting gas flow rates decreases with increasing vacuum chamber pressure.

Many researchers have used physical simulations^[15,18] or industrial tests^[19,20] to determine the circulation flow formula. Nevertheless, each formula is quite different, and the results calculated by different circulation flow formulas are not consistent. It is still meaningful to study the circulation flow rate of specific RH degasser units. In addition, the influence of the ladle bottom stirring process was not considered in the RH degasser circulation flow formulas summarized in previous literature, and the ladle bottom stirring process has a significant effect on RH circulation flow. Therefore, it is useful to add the effect of bottom ladle stirring into the circulation flow. In this paper, the circulation flow rate formula with single-ladle bottom argon plug stirring under the upleg was obtained through physical simulations.

To fit the formula, assume the following: the rising energy of molten steel in the snorkel was mainly provided by the floating work of the bubbles. G_{lif} , H_{imm} , b_{bot} and P_{vac} are independent of each other. The pressure term refers to References 19 and 20. In the fitting process, the relationship between each independent variable and circulate ng flow was regressed to obtain the index. Then, according to the results of the physical simulation experiment, the coefficient of circulating flow is 14.98. The detailed fitting steps are the same as those described in Reference 18. The circulating flow formula is as follows:

$$Q_{cir} = 14.98 G_{lif}^{0.37} H_{imm}^{0.38} b_{bot}^{0.11} [\ln(101325/P_{vac})]^{0.27} \quad [11]$$

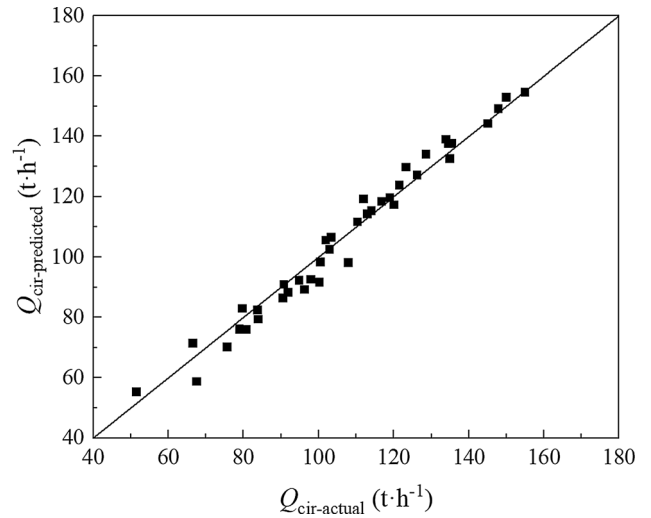


Fig. 7—Predicted data from Eq. [11] vs actual circulation flow rate from the water model.

where b_{bot} is the ladle bottom stirring term, the value is 1 for no ladle bottom stirring, and the range is 2 to 10 $m^3 h^{-1}$ for ladle bottom stirring. G_{lif} ranges from 33.3 to 133.3 $m^3 h^{-1}$, H_{imm} from 0.4 to 0.6 m, and P_{vac} from 133 to 6685 Pa.

The circulation flow formula adopts the data of 40 points. Figure 7 shows the date of predicted circulation flow rate from Eq. [11] and the actual circulation flow rate from the water model. 97.5 pct of data have the error less than 10 pct. It shows that Eq. [11] is reasonable to predict the circulation flow rate.

The formula is fitted according to the variable factors in the simulated factory prototype, without considering the inner diameter of the snorkel. In the formula, lifting gas flow (G_{lif}) and vacuum chamber pressure term $[\ln(101325/P_{vac})]$ are similar to References 19 and 20. Compared with previous studies, this formula takes into account the stirring at ladle bottom, and is more helpful to predict the circulation flow rate of the RH degasser with ladle bottom stirring.

B. Effect of Different Ladle Bottom Stirring Parameters on Mixing Time

Mixing time is an important index for evaluating RH degasser refining efficiency. The shorter the mixing time is, the higher the refinement efficiency of the RH degasser. The mixing time of liquid steel under different ladle bottom stirring processes and lifting gas flow rates was measured, and the prototype parameters were as follows: the immersion depth was 500 mm, the vacuum chamber pressure was 133 Pa, and the other parameters are shown in Table II. The mixing time of double plug bottom stirring, single plug bottom stirring location 1, and location 2 under different lifting gas flows and ladle bottom stirring flows is shown in Figure 8. The figure values are the converted industrial prototype parameter values, and the ladle bottom stirring flow of zero indicates that neither argon plug was stirring the ladle.

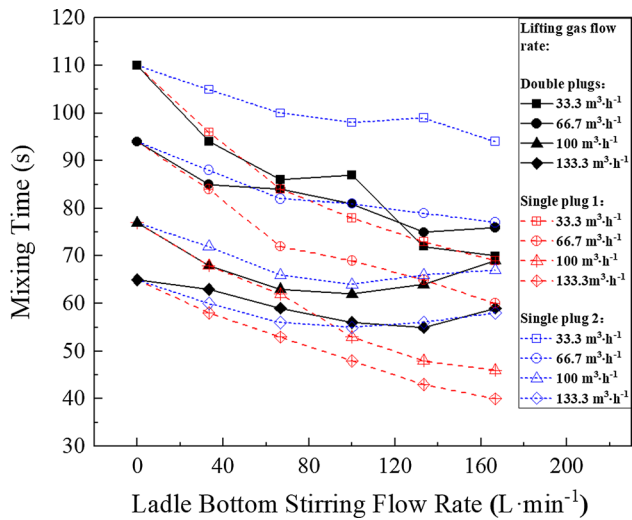


Fig. 8—Variation in mixing time with ladle bottom stirring flow under different ladle bottom stirring conditions and lifting gas flow rates.

Figure 8 shows that the mixing time without ladle bottom stirring is 78 seconds, and the mixing time decreases obviously with increasing ladle bottom stirring. Under the condition of single plug bottom stirring at location 1, the mixing time is slightly lower than that under double plug bottom stirring when the lifting gas flow is $33.3 \text{ m}^3 \text{ h}^{-1}$, and the two plug bottom stirring rates are 33.3 and 133.3 L min^{-1} . Under other experimental conditions, the effect of single plug bottom stirring at location 1 on the mixing time is better. Under single plug bottom stirring at location 1, the mixing time gradually decreases as the ladle bottom stirring flow rate increases under different lifting gas flow rates. When the ladle bottom stirring flow rate is 166.7 L min^{-1} , the mixing time is reduced between 36 and 40 pct compared with no ladle bottom stirring.

Under the conditions of double plug bottom stirring and single plug bottom stirring, when the lifting gas flow rate is 33.3 and $66.7 \text{ m}^3 \text{ h}^{-1}$, the ladle bottom stirring flow rate increases, and the mixing time decreases. When the lifting gas flow rate is 100 and $133.3 \text{ m}^3 \text{ h}^{-1}$, the ladle bottom stirring flow rate increases, and the mixing time first decreases and then increases. The results show that under the condition of a large lifting gas flow rate and ladle bottom stirring at location 2, the small ladle bottom stirring flow has a positive effect on liquid steel mixing. In contrast, under the condition of a large ladle bottom stirring flow rate, the RH degasser circulation rate is compromised, and the liquid steel mixing effect is also affected.

When ladle bottom stirring under the upleg, the RH degasser circulation rate increases and mixing time decreases with increasing ladle bottom stirring flow rate, which is beneficial to the refining process of RH degasser. However, with the increase of the ladle bottom stirring flow rate, the velocity on the free surface of the ladle increases. Ladle bottom stirring may form slag eye

and cause reoxidation of molten steel. The slag layer behavior was not studied in this study. According to Reference 13, no obvious slag eye was formed in the industrial refining of 150-ton RH degasser using ladle bottom stirring under the upleg, with stirring flow rate of 50 L min^{-1} . Thus, to avoid the generation of slag eye, the range of ladle bottom stirring flow rate still needs further study.

C. Effect of Different Ladle Bottom Stirring Parameters on the Flow Field

Figure 9 shows the velocity measurement results of the central cross-section flow field of the upleg and downleg of the RH ladle under the water model's experimental conditions. The test parameters are as follows: the lifting gas flow rate is $4 \text{ m}^3 \text{ h}^{-1}$, the immersion depth is 125 mm, the vacuum chamber pressure is 97711 Pa, and the ladle bottom stirring flow rate is 2 L min^{-1} . The results in Figure 9 are the measured values of the water model. The corresponding industrial prototype parameter values are shown in Table II.

According to Figure 9(a), when there is no ladle bottom stirring, the maximum velocity of liquid steel flowing out of the down leg is 0.34 m s^{-1} . The liquid steel stream directly rushes to the bottom of the ladle, forming two circulation areas. One is a small circulation between the downleg and the left ladle wall. The circulation velocity decreases by approximately 0.16 m s^{-1} during the collision and lifting process. The other is a large circulation between the downleg and the right ladle wall. Due to the long distance, the capacity dissipation is severe, resulting in a rapid decrease in the liquid steel velocity. An inactive area is formed in the lower right corner of the ladle in Figure 9(a).

Figure 9(b) shows that compared with the case without ladle bottom stirring, the circulation of liquid steel in the ladle under the condition of double-ladle argon plug stirring is changed. The liquid steel stream from the downleg collides with the upflow stream formed by the ladle bottom stirring 2 and becomes turbulent. Ladle bottom stirring 1 produces upward flow, which increases the velocity of liquid steel below the upleg. The velocity of liquid steel between the two snorkels and on both sides of the snorkels increases, effectively accelerating the mixing and reducing the extent of the dead zone.

In Figure 9(c), compared with no ladle bottom stirring, under the condition of single-ladle argon plug stirring at location 1, the small circulation on the left side of the downleg in the ladle disappears, and the liquid steel velocity under the upleg increases rapidly. The inactive area between the ladle bottom and the ladle wall is shown in Figure 9(a), enlarging the circulation range in the ladle. Stirring from ladle plug location 1 can activate the area under the upleg, which is beneficial to increase the circulation flow rate and mixing in the ladle. The streamline distribution of the ladle flow field measured by PIV is similar to the numerical simulation

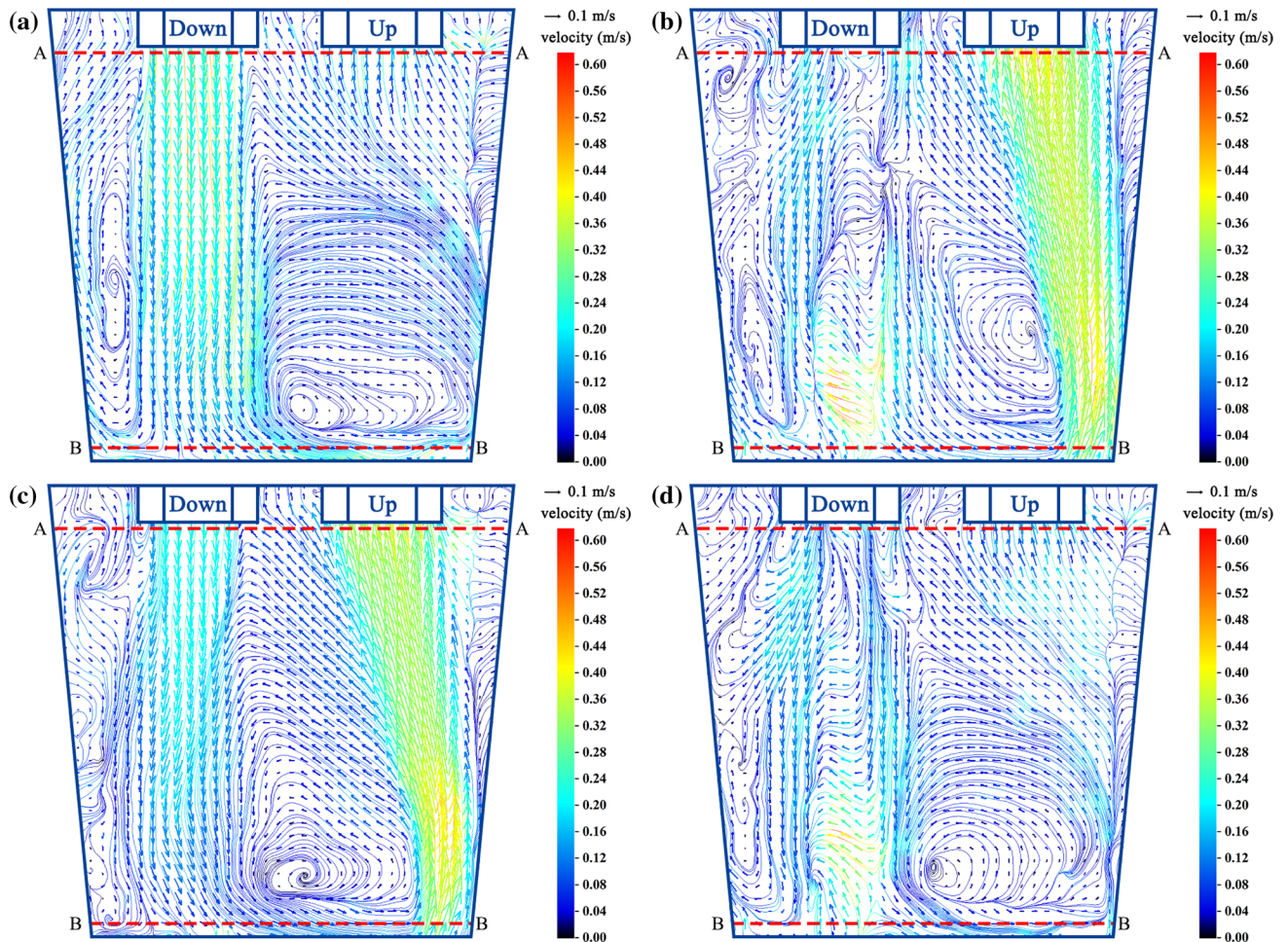


Fig. 9—PIV velocity measurement results of the RH ladle flow field under different ladle bottom stirring conditions: (a) no ladle bottom stirring, (b) double-ladle argon plug stirring, (c) single-ladle argon plug stirring 1, (d) single-ladle argon plug stirring 2.

results of the Reference 8. PIV technology can provide supplement and verification for the numerical simulation.

In Figure 9(d), under the condition of single-ladle argon plug stirring 2, the liquid steel stream from the downleg collides with the upflow stream formed by the ladle argon plug stirring at location 2. The original circulation pattern is greatly affected. The small circulation flow on the left side of the downleg disappears, and the flow velocity at the bottom of the ladle below the downleg is slower. In other words, an inactive area is formed in the lower right corner of the ladle in the figure. Meanwhile, the velocity of liquid steel at the outlet of the two snorkels decreases obviously, which is not conducive to increased circulation flow and a decrease in mixing time.

Figure 9(c) also shows that the ladle argon plug stirring at location 1 below the upleg is beneficial for accelerating the liquid steel entering the upleg, thereby increasing the vacuum vessel circulation flow rate. The ladle argon plug stirring at location 2 below the downleg [Figure 9(d)], where the rising bubble flow impacts the falling liquid steel, hinders the falling liquid steel flow, which is not conducive to improving the circulation flow

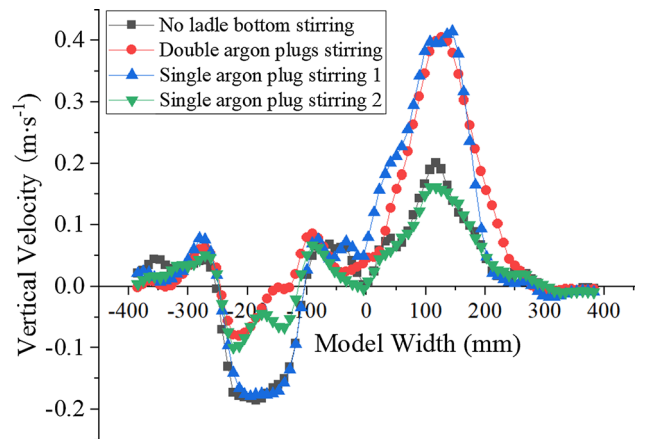


Fig. 10—The vertical velocity distribution of the flow field at Line A-A in Fig. 9(a) to (d).

rate. Nevertheless, because ladle argon plug stirring at location 2 disperses the falling liquid steel, it is conducive to improving the mixing of liquid steel around the falling flow, consistent with the results in Figures 4 and 8.

The flow rate of the molten steel at the outlet of the down leg has an important effect on the circulation flow rate of the molten steel in the RH degasser, which is dotted Line A–A in [Figures 9(a) through (d)]. Therefore, the velocity value at the A–A position is intercepted from the PIV velocity vector diagram, as shown in Figure 10. Figures 9(a) through (d) show that an inactive zone easily forms at the bottom of the ladle during liquid steel circulation. Therefore, the velocity values at dotted Line B–B in the PIV flow field diagram in Figures 9(a) through (d) are selected for comparison, as shown in Figure 11.

Figure 10 shows that the flow velocity under the upleg and downleg is closely related to the ladle bottom stirring operating condition. Compared with the condition without ladle bottom stirring, the maximum downward velocity of liquid steel at the outlet of the downleg decreases from 0.178 to 0.08 m s⁻¹, and the maximum upward velocity of liquid steel at the inlet of the upleg increases from 0.2 to 0.4 m s⁻¹. The reason for this phenomenon is that when other conditions remain unchanged, the gas is injected into the ladle through ladle argon plug 2, and the ascending stream produced by the rising gas has a certain disturbance effect on the descending stream produced by the original circulation of the RH degasser, which makes the original vertical liquid steel stream below the downleg turbulent and reduces the liquid steel velocity at the outlet of the downleg.

Ladle bottom argon stirring at location 1 can increase the liquid steel velocity at the inlet of the upleg, and single-ladle argon plug stirring 2 can decrease the liquid steel velocity at the outlet of the downleg. The velocity of double-ladle argon plug stirring at the inlet of the upleg is similar to that of single-ladle argon plug stirring 1. The velocity of liquid steel at the outlet of the downleg is similar to that of single-ladle argon plug stirring 2. Under the condition of a ladle argon plug stirring of 1, the velocity of liquid steel at the inlet of the upleg and outlet of the downleg is higher, and the flow rate of

liquid steel is better than that under other conditions. This result is consistent with the results of the previous circulation flow experiment.

Figure 11 shows that ladle bottom stirring gives the ladle bottom upward velocity at the ladle argon plug stirring point, as would be expected. Compared with the condition without ladle bottom stirring, under the condition of single-ladle argon plug stirring 1, the upward velocity of liquid steel under the upleg increases from 0.02 to 0.35 m s⁻¹, which reduces the size of the inactive zone between the upleg and the bottom of the ladle. The downward velocity of liquid steel between the downleg and the bottom of the ladle decreases from 0.14 to 0.10 m s⁻¹, which reduces the kinetic energy dissipation caused by the impact of liquid steel on the bottom of the ladle. This shows that the working condition of single-ladle argon plug stirring 1 can reduce the extent of the activation of the inactive zone at the bottom of the ladle and improve the homogeneity and refining efficiency of the RH degasser.

IV. CONCLUSIONS

In this research, a water model was designed based on an industrial size RH degasser of 150 tons. The effects of the ladle bottom stirring flow rate and the number at the location of ladle bottom stirring on the circulation flow rate and mixing time in the RH degasser were studied. The conclusions are summarized as follows:

- (1) Stirring in the ladle bottom argon plug under the upleg enhanced the circulation of the RH degasser ladle system. The velocity of molten steel circulation was accelerated, the RH circulation flow rate was increased, and the mixing time was decreased. When the lifting gas flow rate is 133.3 m³ h⁻¹ and the ladle bottom stirring flow rate is 166.7 L min⁻¹, the circulation flow rate increases by approximately 25 pct, and the mixing time decreases between 36 and 40 pct compared with that without ladle bottom stirring.
- (2) Stirring in the ladle bottom argon plug below the downleg changes the original circulation of the RH flow field. This is not conducive to improving the circulation flow rate but is beneficial to reducing the molten steel mixing time.
- (3) Under the double-ladle argon plug stirring condition, the original circulation of the RH flow field is changed, the flow velocity below the downleg is reduced, the flow is disordered, and the liquid steel activity on both sides of the upleg of the RH ladle is increased appropriately. The working condition of double-ladle bottom argon plug stirring can improve the liquid steel activity on both sides of the upleg, but it negatively affects the RH degasser circulation rate. To ensure that the circulation flow rate will not be reduced, the lifting gas flow must be greater than 133.3 m³ h⁻¹ in the industrial RH degasser prototype studied in this study.
- (4) In this work, it was found that the RH degasser circulation rate increases with increasing lifting gas

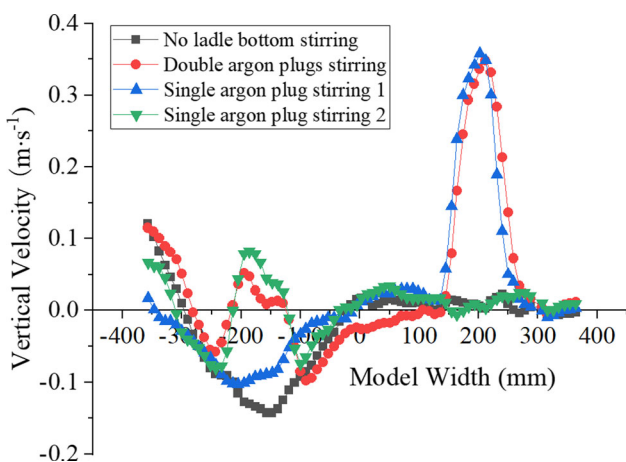


Fig. 11—The vertical velocity distribution of the flow field at Line B–B in Fig. 9(a) to (d).

flow rate, increases snorkel immersion depth and decreases vacuum chamber pressure. With single-ladle argon plug stirring under the upleg, the circulation flow increases with the increasing ladle stirring gas flow rate. A physical simulation is used to fit the circulation flow rate, and the fitting results are as follows: $Q_{\text{cir}} = 14.98 G_{\text{lif}}^{0.37} H_{\text{imm}}^{0.38} b_{\text{bot}}^{0.11} [\ln(101325/P_{\text{vac}})]^{0.27}$.

ACKNOWLEDGMENTS

The authors wish to acknowledge the financial support provided by the National Natural Science Foundation of China (Grant No. U1860106).

CONFLICT OF INTEREST

We declare that we have no financial and personal relationships with other people or organizations that can inappropriately influence our work, there is no professional or other personal interest of any nature or kind in any product, service and/or company that could be construed as influencing the position presented in, or the review of, the manuscript entitled, “The flow behavior of molten steel in an RH degasser under different ladle bottom stirring processes”.

ABBREVIATIONS

| | |
|--------------------------|--|
| g | Acceleration due to gravity (m s^{-2}) |
| u | Characteristic velocity (m s^{-1}) |
| D | Characteristic length (m) |
| d | Diameter (m) |
| ρ_l, ρ_g | Density of liquid and gas, respectively, (kg m^{-3}) |
| Q | Flow rate ($\text{m}^3 \text{s}^{-1}$) |
| $\rho_{l,p}, \rho_{l,m}$ | Liquid density for industrial unit and water model, respectively, (kg m^{-3}) |
| $\rho_{g,p}, \rho_{g,m}$ | Gas density for industrial unit and water model, respectively, (kg m^{-3}) |
| u_p, u_m | Characteristic velocity for the industrial unit and water model, respectively, (m s^{-1}) |
| D_p, D_m | Characteristic length for industrial unit and water model, respectively, (m s^{-1}) |
| Q_p, Q_m | Flow rate for industrial unit and water model, respectively, (m s^{-1}) |
| P | Pressure (Pa) |
| T | Temperature (K) |
| ρ | Density (kg m^{-3}) |
| Q° | Flow rate in standard state ($\text{m}^3 \text{s}^{-1}$) |
| P° | Pressure in standard state (Pa) |
| T° | Temperature in standard state (K) |
| ρ° | Density in standard state (kg m^{-3}) |

| | |
|--------------------------------------|--|
| Q_p°, Q_m° | Gas flow rate of industrial unit and water model in standard state, respectively, ($\text{m}^3 \text{s}^{-1}$) |
| $\rho_{g,p}^\circ, \rho_{g,m}^\circ$ | Gas density of industrial unit and water model in standard state, respectively, (kg m^{-3}) |
| $P_{g,p}, P_{g,m}$ | Gas pressure of industrial unit and water model, respectively, (Pa) |
| P_0 | Standard atmospheric pressure (Pa) |
| P_{vac} | Pressure in vacuum chamber (Pa) |
| h_0 | Vertical distance between the height of water in the vacuum chamber and the ladle liquid level (m) |
| $h_{0,m}, h_{0,p}$ | The h_0 for the industrial unit and water model, respectively, (m) |
| Q_{cir} | Circulation flow rate (t min^{-1}) |
| G_{lif} | Lifting gas flow rate ($\text{m}^3 \text{h}^{-1}$) |
| H_{imm} | Immersion depth of snorkel (m) |
| b_{bot} | Ladle bottom stirring term, the value is 1 for no ladle bottom stirring, and the range is 2 to 10 $\text{m}^3 \text{h}^{-1}$ for ladle bottom stirring (single argon plug stirring under the upleg) ($\text{m}^3 \text{h}^{-1}$) |

REFERENCES

1. D. Mukherjee, A.K. Shukla, and D.G. Senk: *Metall. Mater. Trans. B*, 2017, vol. 48B, pp. 763–71.
2. M. Zhu, J. Sha, and Z. Huang: *Acta Metall. Sin.*, 2000, vol. 36, pp. 763–71.
3. P.A. Kishan and S.K. Dash: *ISIJ Int.*, 2009, vol. 49, pp. 495–504.
4. B.K. Li and F. Tsukihashi: *ISIJ Int.*, 2000, vol. 40, pp. 1203–09.
5. Y. Luo, C. Liu, Y. Ren, and L.F. Zhang: *Steel Res. Int.*, 2018, vol. 89, p. 1800048.
6. C.A. da Silva, I.A. da Silva, E.M. de Castro Martins, V. Seshadri, C.A. Perim, and G.A. Vargas: *Ironmak. Steelmak.*, 2004, vol. 31, pp. 37–42.
7. G.J. Chen and S.P. He: *Vacuum*, 2016, vol. 130, pp. 48–55.
8. D.Q. Geng, H. Lei, and J.C. He: *Ironmak. Steelmak.*, 2012, vol. 39, pp. 431–38.
9. S.P. He, G.J. Chen, and C.J. Guo: *Ironmak. Steelmak.*, 2019, vol. 46, pp. 771–76.
10. K.T. Zhang, H. Cui, R.D. Wang, and Y. Liu: *Metals*, 2019, vol. 9, p. 886.
11. L.F. Zhang and F. Li: *JOM*, 2014, vol. 66, pp. 1227–40.
12. H.T. Ling, C.B. Guo, A.N. Conejo, F. Li, and L.F. Zhang: *Metall. Res. Technol.*, 2017, vol. 114, p. 111.
13. J.D. Dong, C. Feng, R. Zhu, G.S. Wei, J.J. Jiang, and S.Z. Chen: *Metall. Mater. Trans. B*, 2021, vol. 52B, pp. 2127–38.
14. Y. Sahai and T. Emi: *Tundish Technology for Clean Steel Production*, World Scientific, Singapore, 2007, pp. 136–42.
15. L. Lin, Y.P. Bao, F. Yue, L.Q. Zhang, and H.L. Ou: *Int. J. Min. Met. Mater.*, 2012, vol. 19, pp. 483–89.
16. K.L. Bai and J. Katz: *Exp. Fluids*, 2014, vol. 55, p. 1704.
17. H. Cui, J.W. Zhang, J.H. Liu, W. Su, J.B. Yan, and F.L. Wang: *Ironmak. Steelmak.*, 2021, vol. 48, pp. 116–25.
18. S.L. Li, X.G. Ai, N. Wang, and N. Lv: *Adv. Mater. Res.*, 2011, vols. 287–290, pp. 840–43.
19. T. Kuwabara, K. Umezawa, K. Mori, and H. Watanabe: *Trans. ISIJ*, 1988, vol. 28, pp. 305–14.
20. T. Ou, J.G. Liu, J.Y. Zhang, W.Y. Zhou, F.S. Li, and G.Z. Zhou: *Acta Metall. Sin.*, 1999, vol. 35, pp. 411–15.

Publisher’s Note Springer Nature remains neutral with regard to jurisdictional claims in published maps and institutional affiliations.